ENGINEERING RESEARCH INSTITUTE
THE UNIVERSITY OF MICHIGAN
ANN ARBOR

Report No. 2

COMPUTER COMPONENTS DEVELOPMENT

R. T. Denton
W. P. Brown
W. L. Kilmer

Project 2452

NATIONAL SECURITY AGENCY
SIGNAL CORPS PROCUREMENT OFFICE
WASHINGTON 25, D. C.

January 1957

ensn

UMR0576

TABLE OF CONTENTS

	Page
LIST OF ILLUSTRATIONS	iii
ABSTRACT	iv
PULSE-AMPLIFIER ANALYSIS	1
General Qualitative Analysis	1
Resonant-Transformer Analysis	4
Nonresonant-Transformer Analysis	5
Summary	6
PRELIMINARY TRANSFORMER INVESTIGATION	7
Core Materials	7
Core Shape	9
Winding Geometry	10
A. General Procedure	10
B. Test Results	11
C. Core Size	16
Transformer Design Procedure	16
Summary	18
APPENDIX A—ANALYSIS OF STEADY-STATE MAGNETIZING CURRENT IN A TUNED, CRITICALLY DAMPED TRANSFORMER	19
APPENDIX B—ANALYSIS OF RESONANT-TRANSFORMER PULSE RESPONSE	20
APPENDIX C—ANALYSIS OF LIMITATIONS ON RESONANT-TRANSFORMER LOAD CURRENT DUE TO RISE-TIME REQUIREMENTS	23
APPENDIX D—ANALYSIS OF LIMITATIONS ON HIGH-INDUCTANCE TRANSFORMER LOAD CURRENT DUE TO RISE-TIME REQUIREMENTS	25

LIST OF ILLUSTRATIONS

Table		Page
I	Inductance Measurements on Cup-Core Transformers	12

Figure		
1a	Typical pulse-amplifier configuration.	2
1b	Equivalent circuit for pulse amplifier.	2
2	Vacuum-tube plate characteristics.	2
3a	Input signal to grid.	2
3b	Transformer output voltage.	2
4	Relationship of load current to turns ratio for nonresonant transformer.	5
5	Input pulse for transformer tests.	7
6	Core equivalent circuit.	8
7	Test circuit for core B-H measurements.	9
8	Winding configurations.	11
9	Transformer pulse response.	13

ABSTRACT

This report represents preliminary work performed under Phase II of ERI Project No. 2452. The objective of Phase II is complete design information for a pulse transformer applicable to the pulse-amplifier circuitry to be used in Project Bloodhound and an analysis of the frequency limitations and circuit characteristics of the transformer independent of its circuit environment.

The first section of the report is an investigation of the effects of tube, transformer, and external circuit parameters on the output characteristics of tube-transformer pulse amplifiers. Since for the frequency range of interest, the transformer characteristics appear to be independent of frequency, a simplified low-frequency equivalent circuit for the transformer is assumed in this section. Equations are derived which relate the maximum available load current to the circuit parameters and it is shown that a resonant transformer design will allow maximum load current.

The second section of this report is a preliminary study of the limitations on circuit operation imposed entirely by the transformer characteristics. The effects of core material, core size and shape, and winding geometry on transformer characteristics are indicated and some measurements of these effects are presented.

PULSE-AMPLIFIER ANALYSIS

GENERAL QUALITATIVE ANALYSIS

The combination of vacuum tube and transformer exhibits certain fundamental properties when used as a pulse amplifier. It is the purpose of this report to investigate these properties and relate them to circuit capabilities of the tube transformer combination for a particular configuration and type of tube. The configuration considered is shown in Fig. 1a. Figure 1b shows the simplified equivalent circuit which is considered in this analysis. In the simplified equivalent circuit, L is the primary inductance of the transformer, C is the parallel combination of tube plate capacitance, transformer winding capacitance, and reflected secondary capacitance, and R is the secondary load resistance reflected into the transformer primary. It is also assumed that the tube in Fig. 1a has pentode-like plate characteristics as shown in Fig. 2. It should be noted that the tube grid capacitance is neglected in this analysis since we are here concerned primarily with output characteristics of the configuration. Grid capacitance will primarily affect the design of gating structures used to drive the tube. Transformer leakage inductance, coupling capacitance, and core loss also have been neglected as second-order effects.

The output of the tube-transformer configuration with a rectangular pulse on the grid can be derived qualitatively as follows. First, assume the input voltage to the grid is as shown in Fig. 3a. Then, referring to the curves of Fig. 2, the tube will be quiescent at point A with grid voltage e_{g_1} until the pulse arrives at the grid. When the pulse arrives, the grid voltage will immediately increase to e_{g_2} and the plate current, I_p, will jump to I_b with an increase of ΔI. This increment of current will start charging the parallel RC combination in the plate circuit and the operating point will move along the tube characteristic of $e_g = e_{g_2}$ from B to C. The voltage across the plate load at this instant is $(E_b - E_c)$ with a current of $\Delta I'$ flowing through the reflected secondary load, if the assumption is made that the magnetizing current through L has not increased significantly while the parallel RC combination is charging. During the flat-top portion of the pulse, the magnetizing current will be increasing so that the operating point of the tube will be moving back up the characteristic toward the knee. There will be only a slight droop across the top of the pulse as the operating point moves up the curve, as long as the operating point does not go over the knee of the curve. Suppose that by the end of the pulse the operating point is at D. If the grid voltage now drops back to e_{g_1}, the plate current will drop and the tube will be operating at E. The operating point will then move back past A to some point F and drop back to A as the energy stored in the parallel RLC combination is dissipated and the voltage decays. The rate at which the energy is dissipated is dependent on the rel-

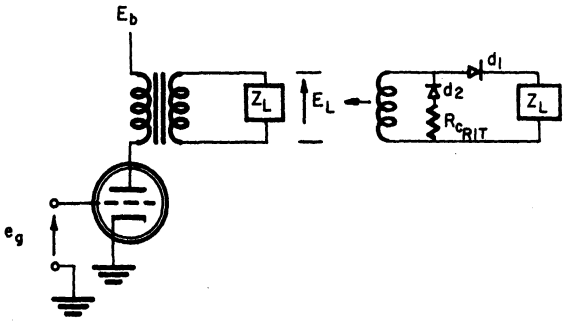

Fig. 1a. Typical pulse-amplifier configuration.

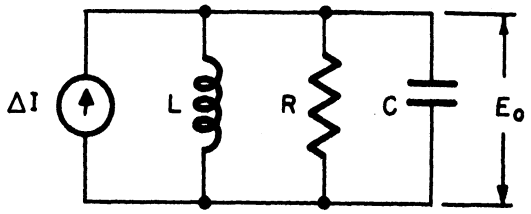

Fig. 1b. Equivalent circuit for pulse amplifier.

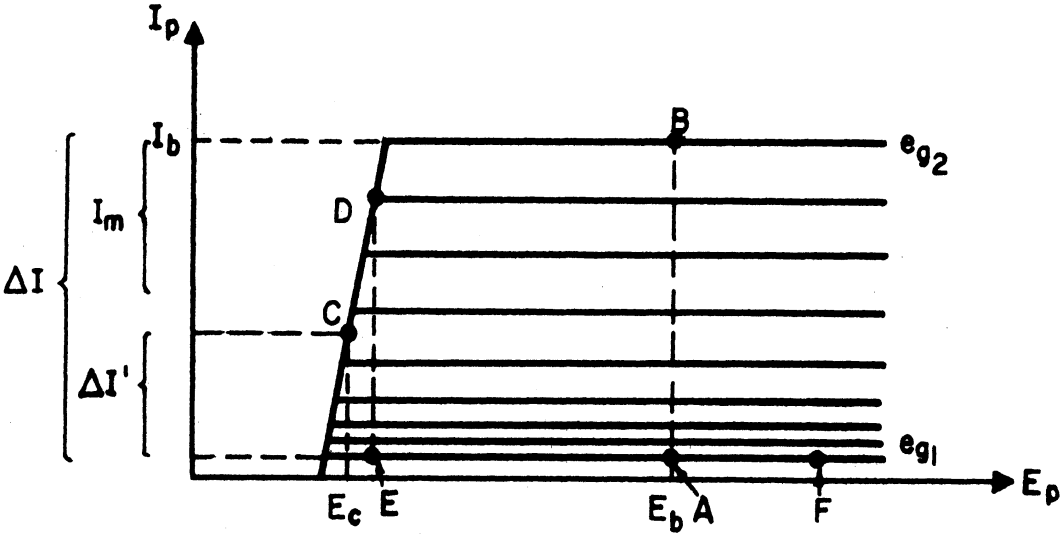

Fig. 2. Vacuum-tube plate characteristics.

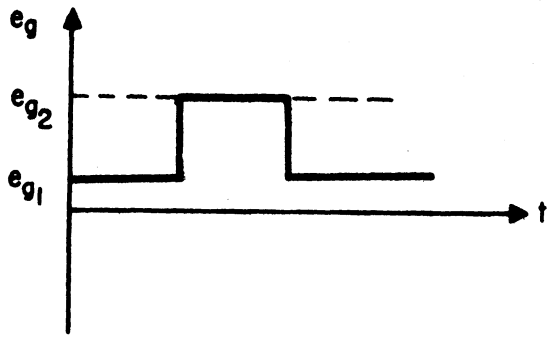

Fig. 3a. Input signal to grid.

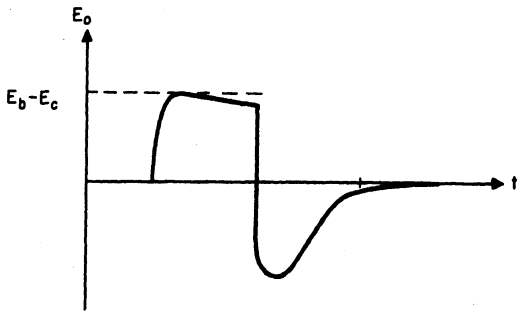

Fig. 3b. Transformer output voltage.

ative values of resistance, capacitance, and inductance. The output voltage also may or may not have an oscillatory decay, depending on whether the system is underdamped or overdamped. Figure 3b, which indicates the voltage response of the transformer primary for a rectangular pulse on the grid, is shown with a critically damped recovery. It can be shown that a critically damped circuit has the fastest possible recovery without overshoot.[1]

It is rather revealing to consider the limitations on transformer output voltage and current due to stray capacitance, tube capacitance, plate current drive, and output pulse shape as they are reflected in the E_p - I_p trajectory of the tube during the pulse interval. If, for example, a certain minimum rise time, τ_1 is specified and a certain output voltage (E_b - E_c) is required, then there will be a minimum R and a maximum C such that the parallel combination can be charged through a voltage (E_b - E_c) in time τ by a current ΔI with the operating point moving from B to C. If R is too small or C is too large, then the operating point will never get to point C and may not even get over the knee of the curve. This will give a reduced output voltage and may cause the pulse to be too narrow. A narrow pulse may also be produced if during the flat-top portion of the pulse the increasing magnetizing current carries the operating point over the knee of the curve. If the operating point goes over the knee, then a slight increase in magnetizing current will drive the operating point back to B and the output voltage will go to zero. There will correspond to a given set of operating conditions a L_{min} which will limit the magnetizing current to a value less than I_m. L_{min} is a function of I_m, E_b - E_c, and τ_2 (pulse width). If L is fixed at some value larger than L_{min}, then by the end of the pulse the tube will be operating at some point D with a magnetizing current less than I_m flowing through the inductance and a voltage E_b - E_c across the capacitor. With given initial conditions and a specified R, L, and C, the output voltage during the recovery time can be calculated quite readily.[2] It can be shown, for example, that recovery time for a given L and C will be shortest with no overshoot when $R = 1/2\sqrt{L/C}$. R can be switched to this value during the recovery time by the proper use of diodes, as will be shown later. The output voltage with critical damping will then be down to $E \simeq 0.01\ (E_b - E_c)$ after a time $\tau = 2\pi\sqrt{LC}$.

We have indicated in this section some of the circuit limitations of the tube-transformer configuration when used as a pulse driving source for an isolated pulse without considering the effects of a train of pulses. The effects of a train of pulses will be important in computer circuit applications since the tube-transformer input may be only an isolated pulse or may be a whole series of pulses, and ideally the pulse output should have the same shape in either case. If the pulse output is not the same in both cases, then the circuit must be designed so that the worst pulse shape, which occurs following a long train of pulses, will still satisfy the minimum output pulse requirements.

---

[1]For more complete discussion of the recovery of a parallel RLC circuit see Millman and Taub, Pulse and Digital Circuits, McGraw-Hill, pp. 52-7.
[2]Millman and Taub, op. cit.

The following two sections are devoted to a qualitative analysis of the further circuit restrictions imposed by the requirement that the tube-transformer be able to act as a driving source for a train of pulses.

RESONANT-TRANSFORMER ANALYSIS

One way to eliminate the pulse-to-pulse interaction due to a train of pulses is to design the transformer so that it will completely recover from one pulse before the next one is present. It can be shown[3] that the minimum recovery time will be $T_{R_{min}} = \pi\sqrt{LC}$ where L and C refer to the elements in the plate circuit of Fig. 1b. If the pulse repetition frequency is f_p, and if the pulses have equal on-off periods, then it follows that for $T_{R_{min}} = 1/2f_p = \pi/\omega_p$, the transformer will just recover during the off pulse period. If we define ω_T, the transformer resonant frequency, as $\omega_T = 1/\sqrt{LC}$, we see that a resonant transformer tuned to the pulse repetition frequency will just recover during the off pulse period. In other words, we require that $\omega_T = 2\pi f_p = \omega_p$, or that the transformer be tuned to the pulse repetition frequency. It turns out that a transformer tune to ω_p will not recover in $1/2f_p$ seconds without excessive overshoot. Overshoot is undesirable because it might cause false triggering, so the transformer must be damped by adjusting R to critical damping. This value of R is given by $R_{crit} = 1/2\sqrt{L/C}$ and can be obtained with a transformer loading scheme as shown in Fig. 1a, where d_1 isolates Z_L during recovery and d_2 switches in R_{crit}. With critical damping the transformer will not completely recover in $1/2f_p$, but the magnetizing current will be reduced to about 0.08 times what it was at the end of the pulse. It is shown in Appendix A that this reduction is enough to make the pulse output relatively independent of the past history of the circuit. The fact that the resonant frequency of the transformer must be greater than the operating frequency sets an upper limit on the transformer inductance for a given capacitance. This condition plus the constraint that the operating point may not go over the knee of the characteristic curve may be used to analyze the operation of a given tube-transformer load configuration. This analysis is carried out in Appendix B and shows that

$$I_{L_{max}} = \frac{23}{140\pi^2}\frac{\Delta I^2}{C_T f_p E_L} - \frac{35\pi^2}{23} f_p E_L C_s \ , \qquad (1)$$

where

I_L = load current referred to the transformer secondary,
ΔI = tube driving current as defined in Fig. 1b,
E_L = pulse output voltage referred to the transformer secondary,
f_p = pulse repetition frequency,
C_T = tube primary capactitance and transformer primary capacitance, and
C_s = transformer secondary capacitance.

[3] Millman and Taub, op. cit.

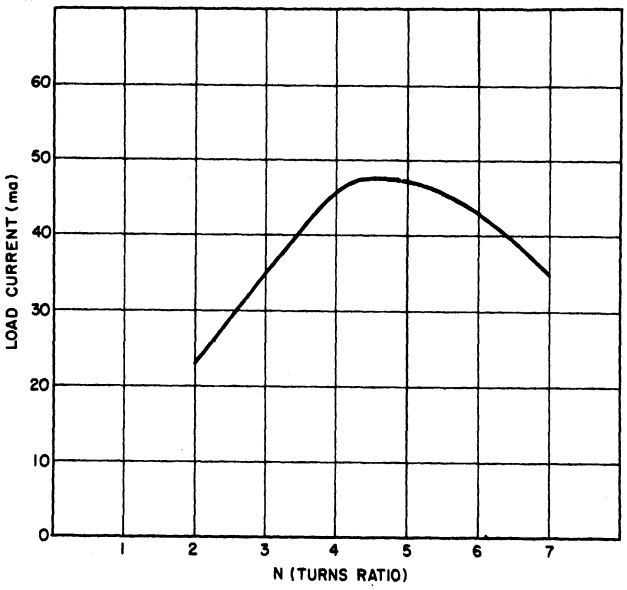

Fig. 4. Relationship of load current to turns ratio for nonresonant transformer.

There is one remaining constraint on the circuit parameters, imposed by the pulse rise-time requirements. As mentioned in the first section of this report, for a given minimum rise time, pulse voltage (E_b - E_c), tube driving current ΔI, and equivalent capacitance, there will be a certain minimum load resistance; which means that there will be a certain maximum load current. An analysis of this situation is developed in Appendix C, giving the relationship

$$I_{L_{max}} = 40\, C_s f_p E_L \ln \frac{\Delta I \sin \pi/10}{4\pi E_L f_p C_T} , \qquad (2)$$

where the symbols have the same meanings as for Equation 1. Thus we see that for particular values of f_p, ΔI, C_s, C_T, and E_L there will be a maximum load current specified by either Equation 1 or Equation 2, whichever is least. It should be noted that, in general, Equation 1 will fix the maximum load current since it gives a lower maximum load current than Equation 2.

NONRESONANT-TRANSFORMER ANALYSIS

It might seem that it would be possible to reduce transformer magnetizing current during the pulse interval and thus increase load current by increasing the transformer primary inductance. This would remove the restriction due to Equation 1 and allow the load current to be fixed by Equation 2. Offhand this would seem like a significant improvement since substitution of typical values for f_p, ΔI, E_L, C_s, and C_T into Equations 1 and 2 shows that Equation 2 would give several times as much load current. This improvement is more apparent than real, however, because the large value of primary inductance will cause a large pulse-to-pulse interaction which puts an additional restriction on the

output load current. The interaction is caused by the transformer-stored energy piling up from pulse to pulse. For large values of primary inductance, only a small amount of energy will be stored per pulse, but only a small fraction of this energy will be dissipated during the off pulse period. This means that for a long train of pulses, stored energy will be accumulating in the transformer until a steady state is reached where the energy stored during a pulse period is equal to the energy dissipated during the off pulse period. For a train of pulses with equal on and off periods, and a large enough inductance so that there will be negligible sag, the steady-state condition will obviously occur when the output voltage during the off pulse period is equal to the output voltage during the pulse period and of opposite sign. This means that for a specified output pulse voltage, E_L, circuit capacitance will have to be charged through $2E_L$, from $-E_L$ to $+E_L$ during the pulse rise time. The nonresonant transformer is analyzed in Appendix D, where the following relation is obtained:

$$e^{-\left[I_L/10f_pE_L(C_s+N^2C_T)\right]} = \left[(N\Delta I/I_L) - 3\right]/\left[(N\Delta I/I_L) - 1\right] \qquad (3)$$

This equation gives a relation between the specified E_L, ΔI, f_p, C_s, C_T, and N and the allowed I_L. Substitution of a range of values for N gives a curve of I_L vs N from which we can select an optimum turns ratio to get maximum I_L. Substitution of typical values for E_L, ΔI, f_p, C_s, and C_T into Equation 1 and Equation 3 will give a comparison of maximum load current for typical resonant- and nonresonant-transformer designs as shown below. Let

$E_L = 5$ v,
$\Delta I = 60$ ma,
$C_s = 50 \times 10^{-12}$ f,
$C_T = 6 \times 10^{-12}$ f, and
$f_p = 5 \times 10^6$ cps.

Then, substitution into Equation 1 gives $I_{L_{max}} = 83$ ma and substitution into Equation 3 for a range of values for the turns ratio gives the curve I_L vs N shown in Fig. 4 so that $I_{L_{max}} = 47$ ma. Thus, a resonant-transformer design would allow a larger load current for circuit values typical of our application.

SUMMARY

Several basic limitations on the circuit operation of the tube-transformer configuration have been discussed. These limitations are independent of transformer core characteristics as long as the characteristics do not deteriorate from their low-frequency values. For ferrite core materials, these characteristics appear to be relatively constant up to and beyond ten megacycles.

On the basis of the basic circuit limitations we have derived several equations which give restrictions on output load current for two different types of

transformer design. The two types of transformer design considered were a low-inductance and a high-inductance transformer. The low-inductance configuration is resonant at the operating frequency. It has been shown that for particular values of circuit parameters, the low-inductance transformer will deliver about twice as much secondary load current. No analysis has been made of any but these limiting cases of primary inductance because of the complexity of the analysis. It seems reasonable to suppose, however, that maximum allowable secondary load current will decrease monotonically as inductance is increased from the resonant value.

It will be the objective of the next phase of the transformer study to determine the frequency limitations and circuit characteristics of the transformer itself, independent of its circuit environment. The second section of this report is a preliminary investigation into some problems involved in this study.

PRELIMINARY TRANSFORMER INVESTIGATION

CORE MATERIALS

There are three characteristics of core materials which are of interest to this research: response time of the core material, core loss factor, and relative permeability. The inherent rise time of the core must be appreciably shorter than any of the rise times associated with the circuit itself. The concept of rise times of core materials arises principally from the inertial property of the elastic walls separating the magnetostatic domains. This elastic wall, or grain boundary as it is sometimes called, can never experience an infinite acceleration. Therefore, the first derivative of the time rate of change of flux and secondary voltage must be a continuous function. Also, the resistivity of the core materials must be high enough to prevent undesirable flux-density lag due to eddy-current shielding. Thus it is apparent that no core material can support a zero rise time.

Rise-time tests were made using the test pulse shown in Fig. 5. Admittedly a much faster rise time should have been used, but this was the best that

Voltage scale:
.5 volts/cm

.1 μsec./cm

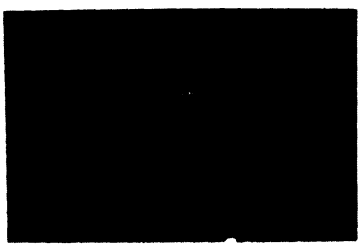

.02 μsec./cm

Fig. 5. Input pulse for transformer tests.

was available at the time. With this test pulse, General Ceramic's Ferramic C, E, G, H, and Q cores all seemed to follow the input perfectly—an indication that all their rise times are at least less than 5 millimicroseconds. One bobbin, wound with only 6 turns to permit a negligible rise time with respect to the winding configuration, was transferrred from core type to core type to keep any effect introduced by the winding the same.

The second core characteristic that must be investigated is closely related in effect to the one just discussed but is distinctly divorced from it in theory. The loss factor, as it is called, is really a measure of the ratio of the real to the imaginary component of the permeability factor. When these real and imaginary permeability components are multiplied by the $j\omega$ frequency term, there results inductive reactance and resistance terms, respectively. Thus the equivalent circuit for the core itself is as shown in Fig. 6.

Fig. 6. Core equivalent circuit.

It should be emphasized that the R in Fig. 6 is an equivalent resistance determined from core loss measurements and <u>not</u> the body resistance of the core. R may be found from the Q of the core at any frequency through the use of the relationship $Q = \omega L/R$. The effect of R is to attenuate the signal being transmitted through the core medium. Since the equivalent R is a function of frequency, the Q of the core is not a linear function of frequency, so tests should be conducted on the core materials available over a range of frequencies to determine where the loss factor of each of the materials becomes prohibitive. Care should be taken to keep the rate of change of flux in the core within about the same range that the eventual circuit voltage and inductance requirements would call for, and few enough turns should be used to reduce stray and leakage parameters to such small values that the rise time of the winding configurations is minimized.

The remaining core characteristic which is of interest is the relative permeability. For all those materials which survive the first two tests, this remains the sole criterion for selection. According to some flux-density calculations and resistivity figures for any core material and shape that we might use, neither overall nor surface magnetic saturation will ever be approached in our application. The surface effects are, of course, brought about at higher frequencies by eddy currents which are small for high-resistivity ferrites in the frequency range of interest to this project. This means that effective permeability over an entire pulse is a function of $d\phi/dt$ (or dB/dt), ΔB, the duration of the pulse, and the steady-state biasing current through the windings. The circuit that has been constructed to test these relationships is shown in Fig. 7. The

$$\int_0^T \frac{V_1 dt}{N} = \Delta B \quad ,$$

where N is the number of primary turns and V_1 and T are the quantities indicated in Fig. 7, is easily obtained from pictures of the voltage, V_1'. The inductance of the coil on the core is the slope of the current rise through R. This follows from the relation $e = L(di_L/dt)$. Since L is directly proportional to the effective permeability and the square of the number of turns, L/N^2 gives a permeability index which is convenient to use in actually designing a transformer. The actual testing of the core materials is still in its first stages and is being held up until more materials arrive. Until the above tests are completed, the manufacturer's values of permeability will be used in the design of test transformers.

CORE SHAPE

It is the purpose of this section to indicate several important principles in the design of an optimum core shape.

To begin with, two necessary characteristics of short-rise-time transformers are small leakage inductances and low distributed capacitances. To achieve the former, the primary and secondary coils must all be kept within a small distance of each other. Tests show that leakages of about 20% of primary inductance occur when a 40-turn primary[4] and two 10-turn secondary windings are placed adjacent to each other on a toroid of .500-in. diameter and .250-in. x .110-in. cross section. This and routine calculations concerning leakage fields between concentrically wound coils mean that the window area through which the winding is placed must be kept both small in height and short in length. Furthermore, the cross-section shape of the core at the winding location should have a maximum area-to-perimeter ratio in order to minimize stray capacitance and leakage inductance for any particular fixed primary inductance and core shape external to the winding section. This is because inductance is directly proportional to the effective $\mu A/\ell$ of the magnetic flux path, and stray capacitance and leakage inductance are directly proportional to the area of the cylindrical winding surface. These considerations can but

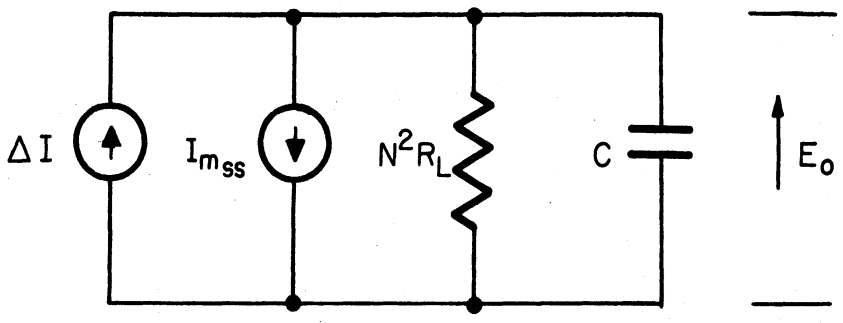

Fig. 7. Test circuit for core B-H measurements.

[4]This gave 200-μhen primary inductance.

specify a cylindrical core shape in the winding region, and a minimum reluctance consistent with the window area requirements for the rest of the magnetic path length.

WINDING GEOMETRY

A. General Procedure.--The research on the various winding geometries was directed at answering one question: how could the cylindrical winding cross section be wound to give the transformer a minimum rise time or otherwise optimal rise time characteristic for any specific wire size, turns ratio, and primary inductance?

It can be shown from simple calculations using typical currents that 34-gage wire is needed in the primary of the transformer if a 416A tube is used, and 35-gage wire is sufficient if a 437A is used. This allows for a .5 duty factor. Wire of 31 gage in the secondaries would allow slightly less than rated current to flow in these windings for a 3:1 turns ratio, 30 gage for a 4:1 turns ratio, etc.

The only sure way to arrive at any conclusions is somehow to isolate, and measure the effects of, each of the stray and leakage terms for each of the winding geometries and converge on the optimum scheme from the information obtained. A great deal of effort has been expended and a great many test runs have been conducted in an effort to do this, but eventually the task was resigned as too difficult to be practical. The mutual and leakage inductances were easily obtained on a Q-meter to within a few percent of their respective values, but the primary-to-secondary capacitance associated with the coils along which voltage gradients exist could only be guessed at from low-frequency (to eliminate the effects of inductance) capacitance bridge measurements. Since this capacitance is proportional to voltage squared, any direct measurements of effective stray capacitance would have had to be made at the same voltage levels as would be used in the final circuit. Furthermore, any measurement of the distributed capacitances associated with the primary and secondary windings will necessarily involve high-frequency inputs and rough calculations show that frequencies well above a kilomegacycle would have to be used in open and shorted secondary tests in order to lump the capacitance effects sufficiently to obtain measurements accurate to within 10 to 15%. Even if good measuring techniques were available at such frequencies, the results could not be relied on very heavily. The reason is that at 1 kilomegacycle, a quarter wavelength of a sine wave, which is the difference between zero and peak voltage, is only 7.5 cm, and the low-frequency circuit approximation that the time necessary to propagate the electromagnetic effects of an a-c signal over the entire circuit is a negligible portion of the period would not be valid.

For a time it was wondered whether or not studies on transformers whose stray capacitances were purposely exaggerated would be of much value, but a few tests seemed to show fairly conclusively that extrapolation of performance

characteristics by dimensional variations on any one winding scheme beyond fairly narrow limits would be meaningless due to the inherent nonlinearity of the situation.

It was finally decided that the most feasible method of arriving at an optimal winding geometry would be simply to wind and test the various schemes with the fastest rising test pulse that could be obtained. The results of this procedure are given in the next section.

B. Test Results.—At this writing, seven basic winding geometries have been tested. It is believed that they represent all the essentially different types that could be devised for a cylindrical winding window. They are shown in Fig. 8. In each case the primary and two secondary windings have their two terminals labeled for convenient orientation in the circuits of Section II. A minus sign on any terminal indicates that that terminal undergoes a voltage drop during the application of a pulse, and a plus sign, a voltage rise. It is not intended that the number of circles should indicate the number of turns of wire, but rather the relative placement of these turns. In Fig. 8(7), it is intended to specify that the primary and negative-going secondary are intertwined and wound together. This scheme, which was suggested by Clark Benson, would of course have its greatest promise in the case of a 1:1 turns ratio where the coupling capacitances would theoretically become zero, but is a sound enough design in general to warrant investigation at higher turns ratio also.

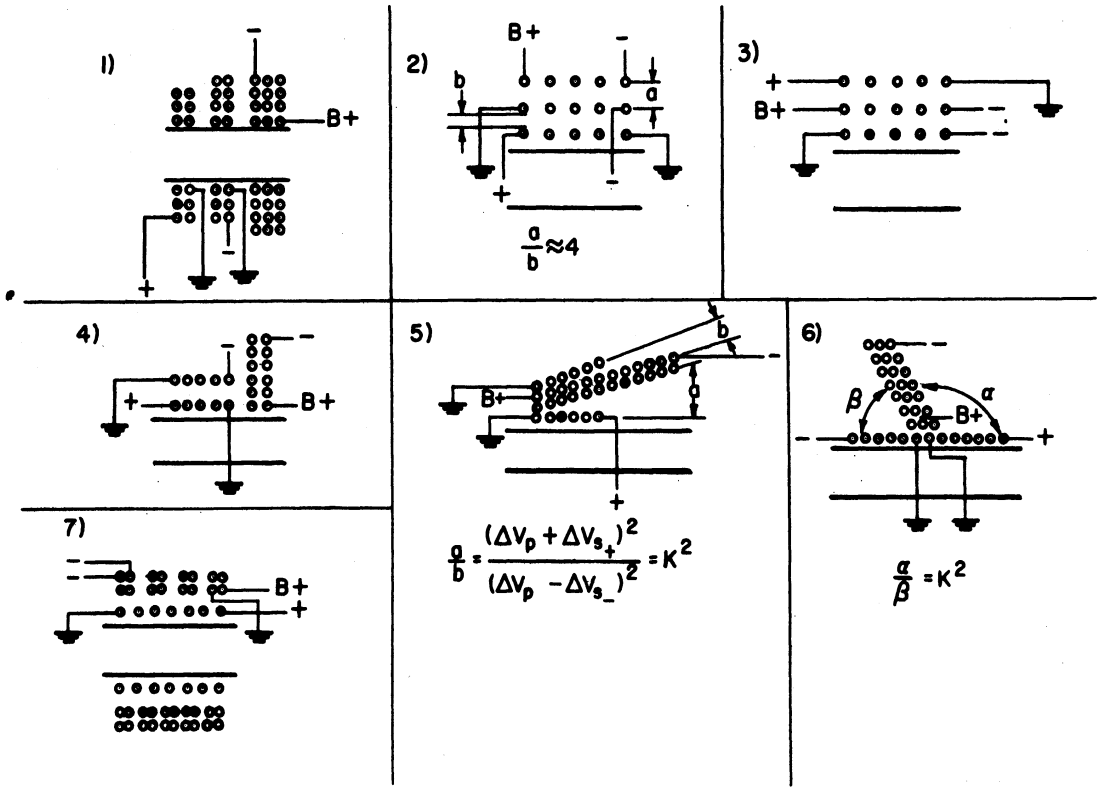

Fig. 8. Winding configurations.

The best-looking test pulse that was available for the rise-time tests is shown in Fig. 5. With this test pulse as an input, the secondary responses to transformer types 1-6 are given in Fig. 9 for several different turns ratios. In each case the negative-going secondary (shown as "-" in Fig. 8) is loaded with 120Ω and the positive-going secondary with 280Ω. Figure 9-1 to 9-6 are for 16:4:4 turns-ratio transformers; 9-7 to 9-12, for 24:6:6; and 9-13 to 9-18, for 32:8:8. The types of windings in Fig. 9 follow one another according to their respective numbers in Fig. 8 for types 1 through 6.

The pictures in Fig. 9 show a distinct overall superiority of winding types 3 and 5. Pictures 9-1 to 9-6 do not show any appreciable difference in the response characteristics, so nothing comparative can be derived from them. It is expected, however, that here again winding types 3 and 5 are the best. As soon as a better test pulse is available (which should be soon), more can be learned about the cases with fewer turns. It might happen, as Fig. 9-17, for example, tends to suggest, that with different numbers of turns the relative desirability of any one type of winding scheme is either increased or diminished. Nevertheless, at present, the third type of winding geometry is clearly the best choice, since its response is as good or nearly as good as any of the others, and it would be much easier to wind mechanically.

The accompanying inductance chart (Table I) gives primary and leakage inductance values for all the 16- and 32-turn cup-core transformers. General Ceramics type-Q core material was used in every case to insure that the core itself did not affect the rise time.

TABLE I. INDUCTANCE MEASUREMENTS ON CUP-CORE TRANSFORMERS

Transformer No.	Primary Inductance = L_p	Leakage to Positive Secondary	Leakage to Negative Secondary	Total Effective Leakage = L_L	$\frac{L_L}{L_p}$ 100%
	In Microhenries				
16:4:4 Turns Ratio					
1	99	7.10	4.93	4.26	4.30
2	71.2	4.90	3.75	3.36	4.72
3	85.5	3.95	2.67	1.82	2.13
4	94	5.70	5.50	4.42	4.70
5	85.5	3.66	2.78	1.55	1.81
6	68.7	3.81	3.42	2.43	3.54
7	----				
32:8:8 Turns Ratio					
1	378	21.3	13.2	12.4	3.28
2	246	16.8	12.9	12.7	4.96
3	385	9.04	5.62	3.42	0.89
4	376	17.45	15.15	13.3	3.54
5	301	9.71	9.18	4.73	1.57
6					
7	---				

Time →

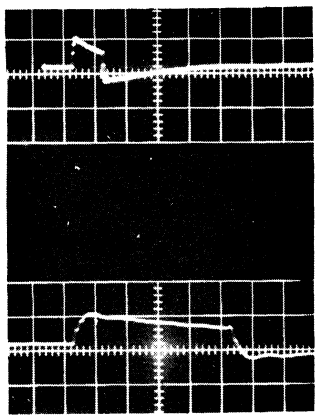

.1 μsec/cm
7 v/cm

.02 μsec/cm
7 v/cm

9-1

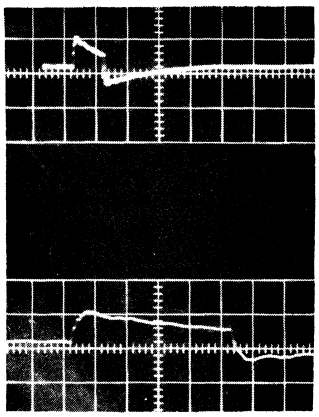

9-2

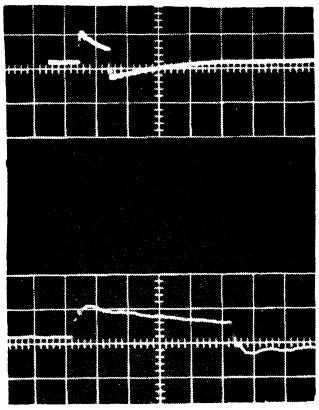

.1 μsec/cm
7 v/cm

.02 μsec/cm
7 v/cm

9-3

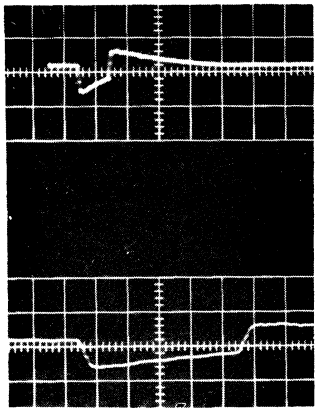

9-4

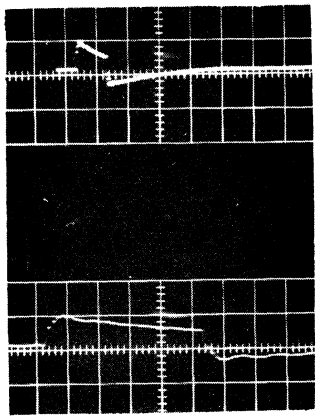

.1 μsec/cm
7 v/cm

.02 μsec/cm
7 v/cm

9-5

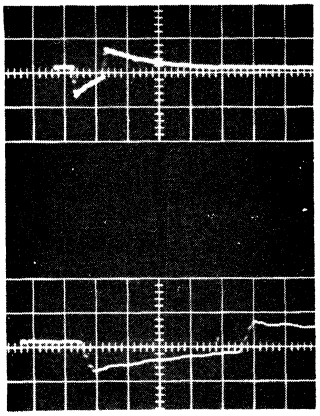

9-6

Fig. 9. Transformer pulse response.

Time →

.1 μsec/cm
7 v/cm

.02 μsec/cm
7 v/cm

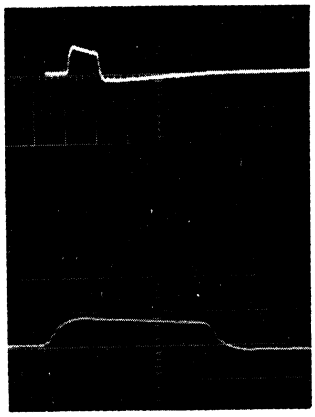

9-7

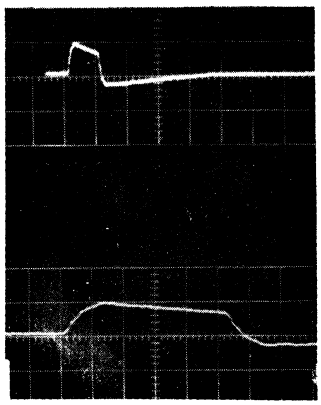

9-8

.1 μsec/cm
7 v/cm

.02 μsec/cm
7 v/cm

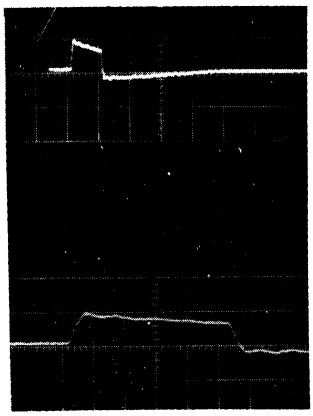

9-9

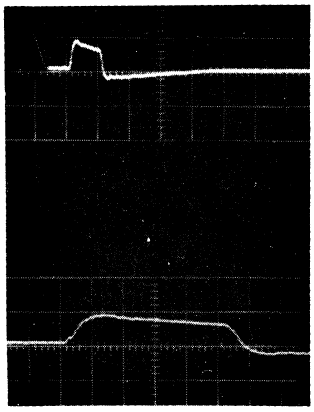

9-10

.1 μsec/cm
7 v/cm

.02 μsec/cm
7 v/cm

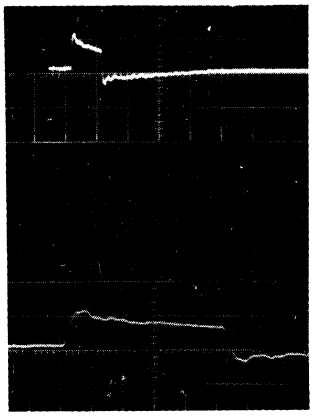

9-11

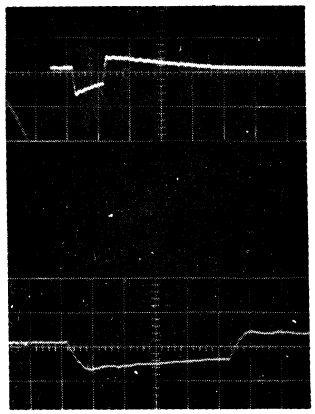

9-12

Fig. 9 (continued)

Time →

.1 μsec/cm
7 v/cm

.02 μsec/cm
7 v/cm

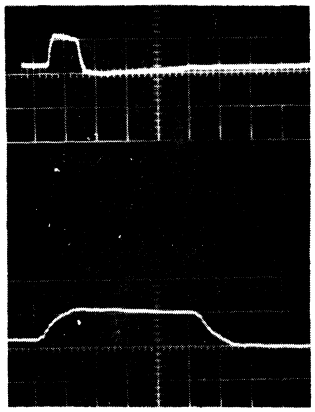

9-13

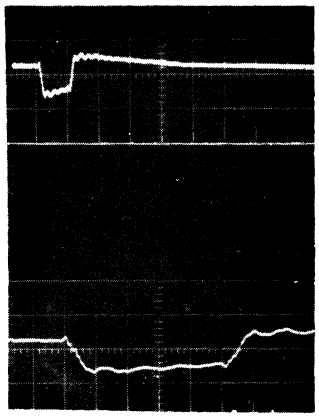

9-14

.1 μsec/cm
7 v/cm

.02 μsec/cm
7 v/cm

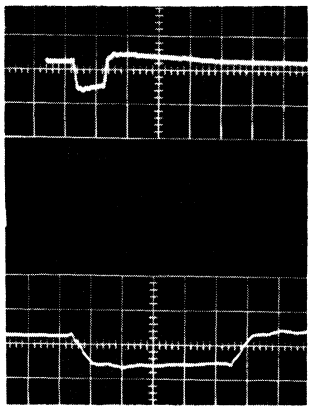

9-15

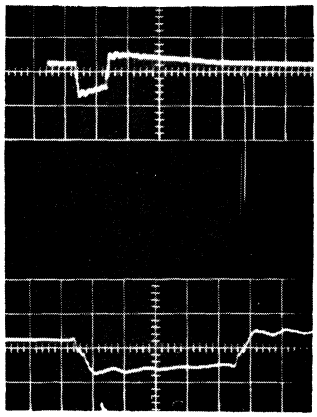

9-16

.1 μsec/cm
7 v/cm

.02 μsec/cm
7 v/cm

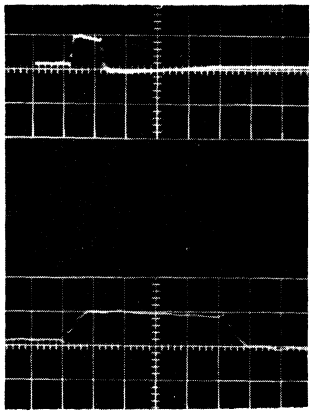

9-17

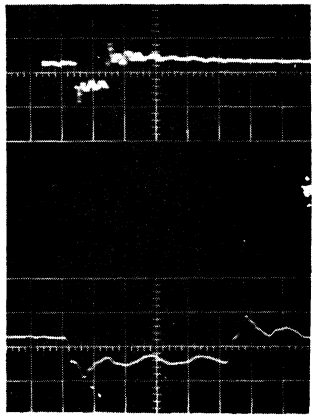

9-18

Fig. 9 (concluded)

The chart and the pictures together re-emphasize the importance of minimizing the leakage inductance and, to a point, the coupling capacitance in obtaining a fast rise time. The other mechanisms which affect the rise time seem quite evident upon reviewing the measurements made on the low-frequency capacitance bridge. That is, the capacitance from primary winding to core is nearly constant at about 1 μμf over all the winding schemes, which means that the effective capacitance is probably just about as constant and considerably less in magnitude. On the other hand, the distributed capacitance associated with the primary coil itself is about .18 μμf for 24 turns of No. 34 wire wound in the manner of winding types 2, 3, and 5, and about .72 μμf for 24 turns of No. 34 wire wound as in type 1. As an illustration of the effect, this and the high leakage inductance explain the relatively poor performance of the first winding scheme. The distributed capacitance along the primary and two secondaries delays the actual transformer action by a slight amount as suggested by the little positive blips before the leading edge of the pulses in Figs. 9-15 to 9-18. From straight capacitance measurements, a set of numbers has been estimated as an indication of the relative coupling capacitance for each of the first 6 winding types (all referred to the first winding type). They are, respectively, 1.0, 4.0, 4.5, 1.3, 4.0, and 1.5. These merit figures correlate with the pictures to suggest that as long as the effective coupling capacitance is kept small, the leakage inductance is the predominate factor limiting the rise of the pulse.

Some additional principles which have been noted in the tests can be stated as follows. (1) The bigger the area of the core at the winding cross section, the less the percentage leakage inductance. This of course is because a greater percentage of the H-field strength exists within the core material for the bigger cross sections. (2) The $Q = \omega L/R$ factor of a primary winding in a cup core fastened together by a screw through its center rises, peaks, and then falls with increasing screw tightness. The inductance of the coil behaves similarly. The explanation is that the magnetic properties of the core are altered as soon as the cores are stressed. (3) Finally, as would be expected, the leakage inductance does not vary noticeably with screw tightness.

C. Core Size.—The test results presented in the preceding section will, when they are completed with better test pulses, specify which winding geometry should be used. This together with the wire sizes called for by the final circuit would completely define the winding dimensions. Then, if some relationships between rise time and winding-region core cross-sectional area are derived, an optimum set of core cross-sectional dimensions can be obtained.

TRANSFORMER DESIGN PROCEDURE

There is a question in engineering research which is often as tantalizing as several other purely technical questions put together. That is: how can the research results be presented to permit the most convenient use of the

knowledge obtained in them if an appreciably different design should be required at some date long after the research is finished. With this in mind, a transformer design procedure has already been established so that the test results and curves obtained can be transformed into design language. The design steps are given below in their natural order:

1. From the rest of the circuit characteristics, derive a turns ratio and the required primary inductance.

2. Select the core materials with short enough rise times and low enough loss factors to permit them to be used at the particular frequencies in question.

3. Calculate

$$\frac{V_p}{An_p} = \frac{\partial B}{\partial t}\text{ avg}$$

where V_p = primary voltage swing,

n_p = number of primary turns,

A = effective cross-sectional area of core $= \dfrac{\sum_i \ell_i A_i}{\sum_i \ell_i}$, where A_i = area over the length ℓ_i, and $\frac{\partial B}{\partial t}$ avg = average rate of change of flux density in gauss,

over the top of the pulse. For the resulting $\partial B/\partial t$, refer to L_p vs n_p charts (L_p = primary inductance) for all the core materials that survive the second design step above. Use only those charts made up for the pulse duration which is to be used. Select the core material that requires a minimum n_p for the desired L_p and $\partial B/\partial t$. This of course will minimize the leakage inductances and stray capacitances and will permit the fastest-rising transformer. All the materials should have separate charts for each of several pulse durations within the range of .1 to .005 μ sec at each of 3 different flux-density biases in order to define it reasonably well. These different biases are especially important in our application because it is contemplated that a quiescent tube current of about 15 ma will flow in the primary winding.

4. Choose the best winding geometry for the number of turns and sizes of wire needed and construct the transformer with the specified bobbins and insulation materials.

The above procedure was formulated under the assumption that the pulse shapes which were to be used would sufficiently closely approximate the test pulse shapes so that for permeability determinations they could be considered the same.

SUMMARY

It is important to note that actually none of the tests thus far have been directed at obtaining the best possible overall transformer that could be constructed with the materials that are currently available. Perhaps the greatest advances that have been made during this phase of Project 2452 have been methodological ones, in that the research has been properly oriented from its several perspectives but few definite decisions have been reached. This report outlines several phases of the transformer problem and indicates the direction of future study. There are some areas left untouched which will be investigated in the future. They include optimum core shape, determination of the optimum leakage-inductance to coupling-capacitance ratio for the best types of winding geometry, and optimum load distribution among the secondary circuits.

APPENDIX A

ANALYSIS OF STEADY-STATE MAGNETIZING CURRENT IN A TUNED, CRITICALLY DAMPED TRANSFORMER

If the magnetizing current increases by an amount I_m during each pulse and is attenuated by a factor K in each interval between, then the magnetizing current at the start of an Nth pulse approaches (as N approaches infinity)

$$\left[(I_mK + I_m)K + I_m\right]K + I_m + \cdots = \frac{I_mK}{1-K} .$$

So, steady-state magnetizing current, $I_{m_{ss}}$, after a long pulse train, approaches

$$I_{m_{ss}} = \frac{I_mK}{1-K} .$$

For a critically damped, tuned transformer, as in the text, where $K \simeq 0.08$,

$$I_{m_{ss}} = I_m \frac{0.08}{1-0.08}$$

$$I_{m_{ss}} = 0.083\ I_m .$$

So, the steady-state magnetizing current will be only about 8.3% of the magnetizing current at the end of one pulse. This means that the output pulse will be essentially independent of the past history of the circuit.

APPENDIX B

ANALYSIS OF RESONANT-TRANSFORMER PULSE RESPONSE

It is assumed that the voltage across the transformer primary during the pulse period has a shape as shown in Fig. B-1 where $\tau_1 = 1/10f_p$, $\tau_2 = 3/10f_p$, and f_p is the pulse repetition frequency. The output voltage during transformer recovery is not shown. In general, magnetizing current in the primary inductance is given by

$$I_m = \frac{1}{L_p} \int_0^T E_o \, dt \quad .$$

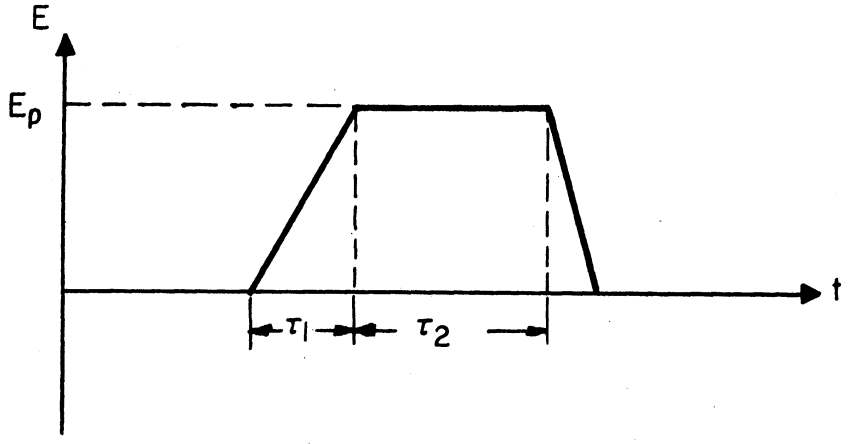

Fig. B-1. Transformer primary voltage.

For the primary voltage shape shown in Fig. B-1, the magnetizing current at the end of the flat-top portion of the pulse is

$$I_m = \frac{1}{L_p} \int_0^{\tau_1} \frac{E_p}{\tau_1} t \, dt + \frac{1}{L_p} \int_0^{\tau_2} E_p \, dt$$

$$I_m = \frac{E_p \tau_1}{2 L_p} + \frac{E_p \tau_2}{L_p}$$

$$I_m = \frac{7 E_p}{20 f_p L_p} \quad .$$

The maximum primary load current, I_{L_p}, will be

$$I_{L_p} = \Delta I - I_m - I_{m_{ss}} ,$$

where

ΔI = plate pulse current and

$I_{m_{ss}}$ = 2/23 I_m as shown in Appendix A for a critically damped transformer.

Further, we have

$$E_p = N E_L$$

and

$$I_{L_p} = \frac{1}{N} I_L ,$$

where E_L = secondary load voltage,
I_L = secondary load current, and
N = primary-to-secondary transformer turns ratio,

so that,

$$I_L = N\Delta I - \frac{7N^2E_p}{20\ f_pL_p} - \frac{7N^2E_p}{230\ f_pL_p} .$$

Since the transformer is tuned to the pulse repetition frequency, we have

$$\omega_p = \frac{1}{\sqrt{L_p\ (C_T + C_s/N^2)}} ,$$

or

$$L = \frac{N^2}{4\pi^2 f_p^2\ (C_s + N^2C_T)} ,$$

so

$$I_L = N\Delta I - \frac{35\ \pi^2}{23} f_pE_L\ (C_s + N^2C_T) . \qquad \text{(B-1)}$$

To find the optimum turns ratio for maximum load current, we take the derivative of I_L with respect to N and set the derivative equal to zero to get

$$N_{opt} = \frac{23\ \Delta I}{70\ \pi^2C_T\ f_pE_L} \qquad \text{(B-2)}$$

Substituting this expression for N into Equation B-1 gives

$$I_{L_{max}} = \frac{23}{140\ \pi^2} \frac{\Delta I^2}{C_T f_p E_L} - \frac{35\ \pi^2}{23} C_s f_p E_L \ . \qquad \text{(B-3)}$$

APPENDIX C

ANALYSIS OF LIMITATIONS ON RESONANT-TRANSFORMER LOAD CURRENT DUE TO RISE-TIME REQUIREMENTS

The pulse rise time of the tube-transformer is analyzed, using the equivalent circuit shown in Fig. 1b. If a current ΔI flows out of the current generator, the primary pulse voltage during the pulse rise time is given by

$$E_o(s) = \frac{\Delta I}{C\left(S^2 + \frac{1}{RC}S + \frac{1}{LC}\right)} ,$$

since it has been shown that $I_{m_{ss}}$ will be negligible. The roots of the quadratic in the denominator are

$$r_1, r_2 = -\frac{1}{2\,RC} \pm \frac{1}{2}\sqrt{\frac{1}{R^2C^2} - \frac{4}{LC}} ,$$

$$r_1, r_2 = -\frac{1}{2\,RC}\left[1 \pm \sqrt{1 - \frac{4R^2C}{L}}\right] ,$$

$$\text{but } L = \frac{1}{4\pi^2 f_p^2\, C} ,$$

so

$$r_1, r_2 = -\frac{1}{2\,RC}\left[1 \pm \sqrt{1 - (2\,RC\omega_p)^2}\right]$$

Let

$$r_1 = -\frac{1}{2\,RC}\left[1 + \sqrt{1 - (2\,RC\omega_p)^2}\right]$$

$$r_2 = -\frac{1}{2\,RC}\left[1 - \sqrt{1 - (2\,RC\omega_p)^2}\right] .$$

Then,

$$E_{o(t)} = \frac{\Delta I}{C\,(r_1 - r_2)}\left(e^{r_1 t} - e^{r_2 t}\right) ,$$

and substituting gives

$$E_{o(t)} = \frac{\Delta IR}{\sqrt{1-(2RC\omega_p)^2}} e^{-\frac{t}{2RC}} \left[e^{\frac{\sqrt{1-(2RC\omega_p)^2}}{2RC}} - e^{\frac{\sqrt{1-(2RC\omega_p)^2}}{2RC}} \right] ,$$

and, since $2RC\omega_p > 1$,

$$E_{o(t)} = \frac{2\Delta IR}{\sqrt{(2RC\omega_p)^2-1}} e^{-\frac{t}{2RC}} \sin \sqrt{\omega_p^2 - (1/4R^2C^2)} \cdot t \quad .$$

However, for typical values,

$$\omega_p^2 \gg \frac{1}{4\ R^2C^2} \quad ,$$

so

$$E_{o(t)} \simeq \frac{\Delta I}{C\omega_p} e^{-\frac{t}{2RC}} \sin \omega_p t \quad . \qquad \text{(C-1)}$$

Then, since $E_{o(t)}$ is required to reach NE_L in $1/10f_p$ seconds,

$$R = N^2 \frac{E_L}{I_L} \quad \text{and} \quad C = \left(C_T + \frac{C_s}{N^2}\right) ,$$

substitution into (C-1) gives the relationship

$$NE_L \simeq \frac{\Delta I}{2\pi \left(C_T + \frac{C_s}{N^2}\right) f_p} e^{-\frac{I_L}{20f_pE_L(C_s+N^2C_T)}} \sin \frac{\pi}{10} \quad .$$

Rearranging gives

$$\frac{2\pi E_L f_p (C_s+N^2C_T)}{\Delta IN \sin \pi/10} = e^{-\frac{I_L}{20f_pE_L(C_s+N^2C_T)}} \quad . \qquad \text{(C-2)}$$

Plots of the left-hand and right-hand sides of this equation show that maximum load current can be drawn when

$$N^2 = C_s/C_T \quad .$$

Substituting this value for N into (C-2) and rearranging gives

$$I_{L_{max}} = 40\ C_s f_p E_L\ \ell n\ \frac{\Delta I \sin \pi/10}{2\ E_L \omega_p C_T} \quad . \qquad \text{(C-3)}$$

APPENDIX D

ANALYSIS OF LIMITATIONS ON HIGH-INDUCTANCE TRANSFORMER LOAD CURRENT DUE TO RISE-TIME REQUIREMENTS

Because of the high primary inductance in this case, the tube-transformer can be represented by the equivalent circuit shown in Fig. D-1. $I_{m_{ss}}$ is given by

$$I_{m_{ss}} = \frac{I_m K}{1 - K} ,$$

as derived in Appendix A. For a transformer with large primary inductance, being driven by a train of pulses with equal on-off intervals, $\tau = 1/2f_p$,

$$I_m = \frac{E\tau}{L} = \frac{NE_L}{2f_p L}$$

and

$$K = e^{-\frac{N^2 R_L}{L}\tau} = e^{-\frac{N^2 R_L}{2f_p L}} .$$

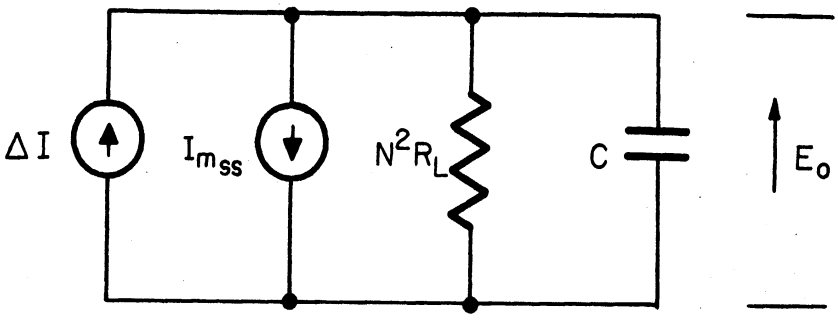

Fig. D-1. Equivalent circuit for nonresonant transformer during pulse rise.

Since

$$\frac{N^2 R_L}{2f_p L} \ll 1 ,$$

$$K \simeq 1 - \frac{N^2 E_L}{2f_L}$$

and

$$I_{m_{ss}} \simeq \frac{E_L}{NR_L} - \frac{NE_L}{2f_L} .$$

However, for large L, the second term is small compared to the first, so

$$I_{m_{ss}} = \frac{E_L}{NR_L} .$$

For the circuit of Fig. D-1

$$E_o = N^2R_L (\Delta I - I_{m_{ss}}) \left(1 - e^{-\frac{t}{N^2R_LC}}\right) ,$$

and since, as is discussed in the body of the report, E_o must rise through $2NE_L$ in a time $\tau = 1/10f_p$, we have the relation

$$2NE_L = N^2R_L (\Delta I - I_{m_{ss}}) \left(1 - e^{-\frac{1}{10N^2CR_Lf_p}}\right) .$$

Then, substituting for $I_{m_{ss}}$ and rearranging terms gives

$$e^{-\frac{1}{10N^2CR_Lf_p}} = \frac{\frac{N\Delta I}{E_L} R_L - 3}{\frac{N\Delta I}{E_L} R_L - 1} ,$$

but since $C = C_T + C_s/N^2$, and $R_L = E_L/I_L$, we have

$$e^{-\frac{I_L}{10E_Lf_p(C_s+N^2C_T)}} = \frac{\frac{N\Delta I}{I_L} - 3}{\frac{N\Delta I}{I_L} - 1} .$$

UNIVERSITY OF MICHIGAN
3 9015 02519 6422